ELSEVIER

Sensors and Actuators A 53 (1996) 273–277

SENSORS AND ACTUATORS A PHYSICAL

A sensitive Pirani vacuum sensor and the electrothermal SPICE modelling

Bruce C. S. Chou *, Yeong-Maw Chen, Mang Ou-Yang, Jin-Shown Shie

Institute of Electro-Optical Engineering, National Chiao Tung University, 1001 Ta Hsueh Road, Hsinchu, Taiwan

Abstract

A sensitive micro-Pirani vacuum sensor has been fabricated. With effective schemes of ambient-temperature compensation and stabilization, it is capable of measuring vacuum pressure linearly from 1 torr down to 10^{-7} torr, a three orders-of-magnitude improvement in resolution over conventional gauges. A special electrothermal SPICE model, complementary to the conventional analog representation of thermal parameters, is also proposed. It allows a high-level sensor-circuit integrated simulation based on the most fundamental principle and thermal variables. Good agreement between the measured data obtained from a constant-temperature readout circuit and the simulation result is demonstrated.

Keywords: Pirani microsensors; Electrothermal SPICE; Constant-temperature circuits; Temperature compensation

1. Introduction

The conventional Pirani gauge is used for vacuum measurement ranging from 10^{-4} to 100 torr. Being of thermal-conductivity type, its working principle is based on the fact that heat loss of a hot object to the ambient is related to the pressure of its surrounding gas. The vacuum pressure can be measured according to the temperature change of a thermally sensitive resistor on the hot object, which is caused by the amount of heat loss. Recently, by using the micromachining technique, some vacuum microsensors much smaller than the conventional types have been developed [1–5]. These include the thermoelectric type [1,2] and the resistive (Pirani) type [3–5]. However, the lowest measurable pressure among these was only limited to 0.1 mtorr [5].

In this paper, we present a highly sensitive Pirani vacuum sensor that is capable of measuring vacuum pressure down to 10^{-7} torr by using a constant-temperature (CT) readout circuit combined with a compensation technique that is able to cancel the ambient-temperature drift effectively. Moreover, a new SPICE model is proposed to account for the pressure-dependent electrothermal characteristics of this Pirani sensor. A simulation concept complementary to the conventional analogy between electrical and thermal parameters [6–9] is to represent the temperature by current, heat capacity by electrical inductance, and thermal conductance by electrical resistance. This analog scheme provides an easier way of representing various thermal-conduction mechanisms in parallel with the ambient, and thus is solvable directly by a SPICE package that uses the most basic thermal parameters, such as pressure and temperature, in simulation.

2. The sensor structure

Fig. 1 shows the schematic diagram and photograph of the fabricated micro-Pirani sensor. It contains a sensing resistor, R_s, on a floating glass membrane and an on-substrate dummy resistor, R_d, for the purpose of ambient temperature compensation. R_s and R_d are made of Pt film simultaneously during processing, and have resistances of 600 and 900 Ω, respectively. The floating membrane is supported by four thermally isolated leads crossing over an anisotropically etched V-groove cavity. The sensor has a square structure with dimensions $A = 4$ μm, $B = 80$ μm and $C = 325$ μm, as depicted in Fig. 1(a).

3. Thermal characteristics

The temperature behaviour of the Pt-film sensing resistor is described by

$$R_s = R_{s0}[1 + \alpha_0(T - T_0)] \quad (1)$$

* Corresponding author. Phone: 886 35 712121 (ext.56317). Fax: 886 35 716631. E-mail: u8024809@cc.nctu.edu.tw.

PII S0924-4247(96)01158-2

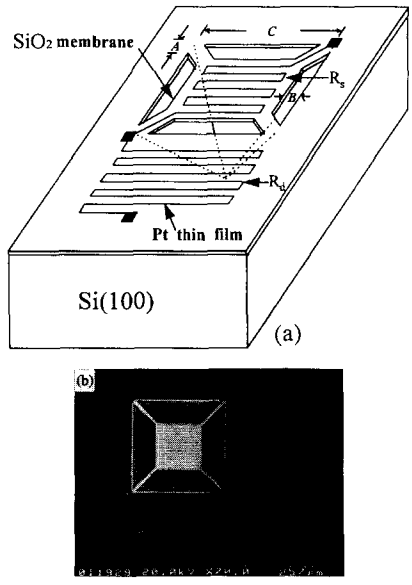

Fig. 1. The structure of the fabricated micro-Pirani sensor: (a) schematic drawing, where A, B and C are the characteristic dimensions of the device; (b) SEM picture with on-substrate dummy sensor.

where R_{s0} is the sensor resistance at a reference temperature T_0, α_0 is its temperature coefficient of resistance (TCR), which is measured to be 0.28% $°C^{-1}$, and T is the temperature on the floating membrane. The high thermal resistance of the lead structure makes the temperature distribution nearly uniform over the membrance surface. This sensor is to be driven by an associated constant-temperature circuit.

According to the conservation of energy, the heat-flow equation of the fabricated Pirani sensor can be represented by a set of lump parameters [5], which reads

$$\mathscr{H}\frac{d\theta}{dt}+\mathscr{G}\theta=\mathscr{P}_e=I_s{}^2R_s \tag{2}$$

where $\mathscr{H}$ and $\mathscr{G}$ are the lump heat capacity and thermal conductance, respectively. P_e is the Joule self-heating power on the sensor, I_s is the current flow through the sensor, and θ is the temperature rise of the membrane above the ambient temperature T_a, namely $T=T_a+\theta$. Eqs. (1) and (2) govern the electrothermal behaviour of the Pirani sensor. Generally, the thermal conductance $\mathscr{G}$ consists of three components: the gaseous conductance ($\mathscr{G}_g$), solid conductance ($\mathscr{G}_s$) and radiative conductance ($\mathscr{G}_r$).

For pressure measurement, the most important term is the gaseous conduction, which reads [5,10]

$$\mathscr{G}_g=KA_sP\left(\frac{P_{tl}}{P+P_{tl}}+\frac{P_{tu}}{P+P_{tu}}\right) \tag{3}$$

where K is a constant related to the properties of the ambient gas molecules; A_s is the sensor area; P is the ambient pressure; finally P_{tl} and P_{tu} are the transition pressures on both sides of the membrane, which are inversely proportional to the effective separations of the membrane from their heat sinks, respectively [10].

An empirical formula for the device solid conductance reported previously by Weng and Shie [5] is written as

$$\mathscr{G}_s=\left(\frac{1}{4.2k_td}\frac{B}{A}+5\times10^4\right)^{-1} \tag{4}$$

where k_t is the effective thermal conductivity (0.0312 W cm^{-1} $°C^{-1}$) and d (0.9 μm) the thickness of the floating membrane. The first term on the right-hand side of Eq. (4) is the thermal resistance of the membrane leads, while the second term is the spreading resistance at the lead end.

The radiative conduction can be represented by [5,11]

$$\mathscr{G}_r=2\epsilon\sigma A_s(T^2+T_a{}^2)(T+T_a) \tag{5}$$

with ϵ the emissivity and σ the Stefan–Boltzmann constant.

4. SPICE modelling

SPICE modelling for thermal microsensors serves two purposes: it provides the convenience of an integrated simulation on both electrical and thermal circuitries simultaneously; also it solves the complicated coupling problems existing between Eqs. (1) and (2) through the feedback scheme that is provided by the electrical circuit method.

To understand and predict the electrothermal characteristics of the related thermal sensors, various equivalent circuits of thermal modelling have been developed recently by many authors [6–9]. However, some SPICE simulations were related to the analysis of the temperature distribution on the sensor surface with the discrete technique [6,7]. Integrated simulation including the thermal and electrical circuits together in a single package has also been developed by a few authors [8,9], with different equivalent sensor models. For the new modelling to be presented in this report, the lumped Eq. (2) is adopted for simplicity of elucidation.

Referring to the above-mentioned lumped thermal parameters, all the conventional electrothermal SPICE modellings have used the analog representation between the sensor thermal parameters and the electrical elements provided by SPICE by the relationships: temperature (T) to voltage (V); heat capacity ($\mathscr{H}$) to electrical capacitance (C); thermal resistance ($\mathscr{R}=\mathscr{G}^{-1}$) to electrical resistance (R); and thermal power, such as the self-heating ($\mathscr{P}_e$) in Eq. (2), to electrical current (I). However, this representation generates the problem of difficulty in dealing with the integrated simulation directly related to Eqs. (3)–(5), which is to be explained below.

The problem originates from the representation of the thermal resistance ($\mathscr{R}$) term, which for the micro-Pirani sensor reads

$$\mathscr{R}=\mathscr{G}^{-1}=\frac{1}{\mathscr{G}_s+\mathscr{G}_g+\mathscr{G}_s}=\frac{1}{\frac{1}{\mathscr{R}_s}+\frac{1}{\mathscr{R}_g}+\frac{1}{\mathscr{R}_s}} \tag{6}$$

If we let $\mathscr{R}_r$, $\mathscr{R}_s$ and $\mathscr{R}_g$ terms be represented by three appropriate electrical resistors as is conventional, then direct

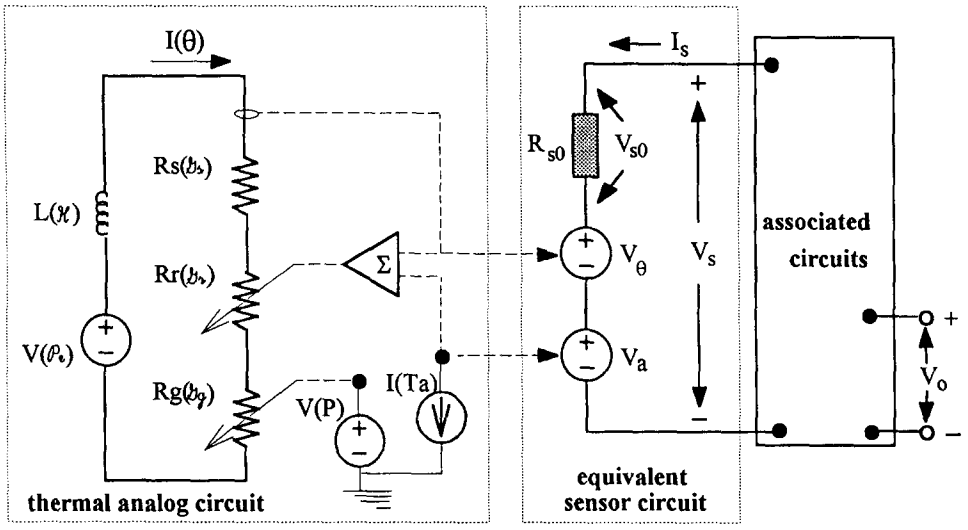

Fig. 2. Equivalent circuit for the proposed electrothermal SPICE model of the Pirani sensor.

use of the most basic variables in Eqs. (3) and (5), such as T and P, for electrothermal SPICE simulation is not feasible, according to Eq. (6). It is necessary to precalculate the value of $\mathscr{G}$ according to the three equations and put it into SPICE before executing the simulation. Hence the procedure becomes very laborious and time consuming.

An alternative concept is developed here to solve the difficulty. It is wise to represent all the thermal conductances here by electrical resistance instead of electrical conductance. The corresponding changes of representation for other parameters are temperature (T or θ) to current (I), heat capacity ($\mathscr{H}$) to electrical inductance (L), and thermal power ($\mathscr{P}$) to voltage (V). This analogy thus appears to be complementary to that of the conventional representation mentioned above.

According to the analogy, the heat-flow Eq. (2) is transformed into

$$L\frac{\mathrm{d}I}{\mathrm{d}t}+RI=V \tag{7}$$

for SPICE simulation. The equivalence of the analog thermal circuit is depicted in Fig. 2 (left dotted box), in which $\mathscr{G}_s$, $\mathscr{G}_r$ and $\mathscr{G}_g$ are expressed in an additive series scheme, as implied in Eq. (2).

Based on Eqs. (3) and (5), $\mathscr{G}_r$ is temperature dependent, which can be further represented by a current-controlled resistance R_r; while $\mathscr{G}_g$ is pressure dependent, which can be represented by another voltage-controlled resistance, R_g, with pressure P as the independent voltage source. The solid conductance $\mathscr{G}_s$ is simply a numerical constant calculable by Eq. (4). Therefore the equivalent RL thermal circuit can be coupled directly to the associated readout electronics for performing the simulation in a single SPICE package, which the conventional representations cannot achieve.

When the sensor is driven by an external associated circuit, the voltage drop on the sensor, according to Eq. (1), can be expressed by

$$V_s=I_sR_{s0}\{1+\alpha_0[(T-T_a)+(T_a-T_0)]\}$$
$$=I_sR_{s0}+\alpha_0I_sR_{s0}\theta+\alpha_0I_sR_{s0}(T_a-T_0)=V_{s0}+V_\theta+V_a \tag{8}$$

where

$$V_\theta=\alpha_0I_sR_{s0}\theta \tag{9}$$

and

$$V_a=\alpha_0I_sR_{s0}(T_a-T_0) \tag{10}$$

are represented by two current-controlled voltage sources (CCVSs). Each CCVS is affected by the sensor current I_s, and an analog current I, which represents either the temperature rise θ, or the ambient temperature T_a. These are depicted in the middle dotted box of Fig. 2.

As shown in the Figure, θ is influenced by the three thermal conduction mechanisms, which in turn are effected by θ. Therefore a complicate electrothermal feedback behaviour appears to exist in such a simple resistive thermal device, which is also implied in Eqs. (1) and (2).

In summary, RL circuit components and some current- or voltage-controlled voltage sources are used to represent the thermal parameters of the micro-Pirani sensor. The model established is thus capable of carrying out the integrated electrothermal simulation by direct substitution of the basic thermal variables into the SPICE package.

5. Experiment and results

The fabricated sensor is driven by a constant-temperature (CT) circuit that was used by Mastrangelo in a microbridge study [8]. As shown in Fig. 3, a matching pair of n-channel JFETs in saturation mode is used as a pair of voltage-controlled current sources, and the output voltage V_o is measured. During the operation, the instrumentation amplifier (AMP-02) forces the voltage drop on the sensor R_s tracking that on

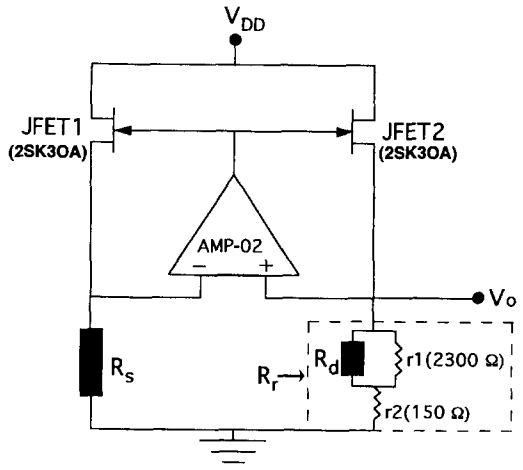

Fig. 3. The CT circuit used in this experiment. R_r is the reference resistor, which is composed of a dummy element, R_d, and two constant resistors, r_1 and r_2, for ambient-temperature compensation.

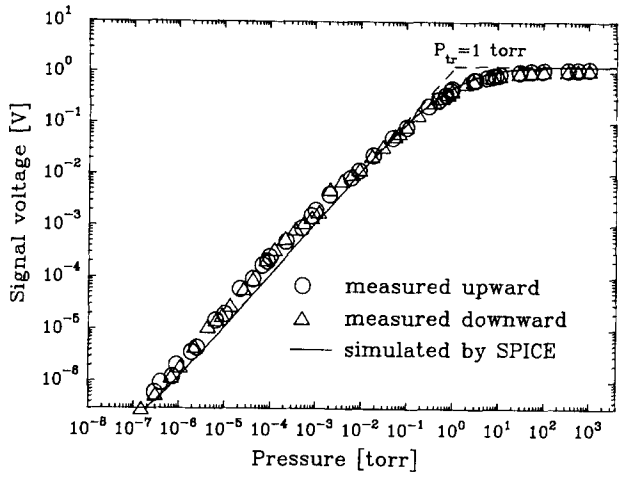

Fig. 4. The measured data of the experiment (triangles and circles), and the simulation result (solid line) by the present electrothermal SPICE model. Notice that a lowest detectable pressure of 10^{-7} torr can be obtained reversibly, and the good agreement between the experiment data and the simulation results.

the reference resistor, R_r. Since the JFET pair is matched, the approximation $R_s \approx R_r$, namely the quasi-constant resistance (or -constant temperature) on R_s, can be achieved. It is worth noting that R_r is composed of an on-chip dummy resistor, R_d, and two temperature-independent resistors, r_1 and r_2. This composition, as reported previously [5,12], is used to reduce very effectively the ambient-temperature drift. Furthermore, a TE-cooling thermostat is used to control the sensor substrate temperature, which is close to that of the ambient, to the extent of 23 ± 0.001 °C in long-term stability [13]. Combining these two methods of temperature compensation and stabilization discussed above, it is able to reduce the ambient voltage drift down to less than 1 μV at output. This is extremely important for the signal measurement, in which the ambient significantly influences the detection resolution.

The assembled sensor module is installed inside a vacuum chamber, which is evacuated down to 10^{-8} torr to serve as the calibration pressure [5]. Nitrogen gas is fed through a needle valve into the chamber for the adjustment of the chamber pressure, which is monitored by a commercial Pirani gauge and a cold-cathode gauge (Balzers TPG-300) for the low- and high-vacuum domains, respectively. The output signal of the CT circuit, V_o, is first nulled at the calibration pressure, then the acquired data read by a high-resolution digital voltmeter (DVM) while the pressure is varied. Signals are sampled and recorded by a PC through a GPIB interface.

Fig. 4 shows the measured data (circles and triangles) for the assembled Pirani gauge, indicating that a linear range between 1 torr and 1×10^{-7} torr is obtainable reversibly. The solid line is the simulation result from the electrothermal SPICE modelling as proposed in the above section. It shows good agreement with the measured data. It is also possible to determine through our SPICE simulation fitting that the effective transition pressure in Eq. (3) is about 1 torr. This value mainly arises from the smaller equivalent separation from the membrane to the V-groove surface, which is estimated to be 60 μm [5]. The transition pressure is the limiting factor for the upper bound of pressure measurement. A wider linear range can be achieved by reducing the above equivalent spacing through structure and process modifications. Linear pressure measurement up to nearly one atmosphere is possible if the separation could be reduced to less than 0.5 μm, according to the theoretical analysis [10].

One should also note that a lowest detectable pressure of 10^{-7} torr has been achieved by the experiment, which is three orders of magnitude more sensitive than conventional Pirani vacuum gauges. The sensitivity is contributed by the extremely low solid conductance (less than 10^{-6} W °C^{-1}), which is nearly radiation limited; the large active area for the enhanced gaseous conduction, compared to the microbridge type used in other work [3]; and finally the effective cancellation of ambient drift by our partial dummy method.

6. Conclusions

A sensitive micro-Pirani sensor having the capability of detecting pressure down to 10^{-7} torr is discussed in this paper. A new electrothermal SPICE model using the appropriate parameter representation is introduced, which provides a feasible high-level integrated simulation of the sensor performance based directly on the fundamental variables, and results in good agreement between the measurements and the simulations. In principle this model is equally applicable to the other types of resistive thermal device, such as flow sensors and microheaters, in which thermal-conduction loss mechanisms are in parallel to the ambient.

Acknowledgements

This study is supported by National Science Council of the Republic of China under project contract No. NSC-82-0404-E-009-127.

References

[1] A.W. Van Herwaarden and P.M. Sarro, Integrated vacuum sensor, *Sensors and Actuators, 8* (1985) 187–196.

[2] A.W. Van Herwaarden and P.M. Sarro, Floating-membrane thermal vacuum sensor, *Sensors and Actuators, 14* (1988) 259–268.

[3] C.H. Mastrangelo and R.S. Muller, Microfabricated thermal absolute-pressure sensor with on-chip digital front-end processor, *IEEE J. Solid-State Circuits, 26* (1991) 1998–2007.

[4] A.M. Robinson, P. Haswell, R.P. Lawson and M. Parameswaran, A thermal conductivity microstructural pressure sensor fabricated in standard complementary metal–oxide semiconductor, *Rev. Sci. Instrum., 63* (1992) 2026–2029.

[5] P.K. Weng and J.S. Shie, Micro-Pirani vacuum gauge, *Rev. Sci. Instrum., 65* (1994) 492–499.

[6] N.R. Swart and A. Nathan, Flow-rate microsensor modelling and optimization using SPICE, *Sensors and Actuators A, 34* (1992) 109–122.

[7] S.B. Crary, Thermal management of integrated microsensors, *Sensors and Actuators, 12* (1987) 303–312.

[8] C.H. Mastrangelo, Thermal applications of microbridges, *Ph.D. Dissertation*, U.C. Berkeley, (1991).

[9] N.R. Swart and A. Nathan, Coupled electrothermal modeling of microheaters using SPICE, *IEEE Trans. Electron Devices, 41* (1994) 920–925.

[10] S. Dushman, *Scientific Foundations of Vacuum Technique*, Wiley, New York, 2nd edn., 1962, p. 39.

[11] R.H. Kingston, *Detection of Optical and Infrared Radiation*, Springer, Berlin, 1978, p. 89.

[12] J.S. Shie, B.C.S. Chou and Y.M. Chen, High performance Pirani vacuum gauge, *J. Vac. Sci. Technol.*, to be published.

[13] U.C. Chang, The application of compensated feedback temperature control to optoelectronics devices, *Master's Thesis*, National Chiao-Tung University, Taiwan (1993).

Biographies

Bruce C. S. Chou received his B.S. degree in physics from Tung Hai University of Taiwan in 1989, and his M.S. degree in nuclear science from National Tsing Hua University in 1991, majoring in high-vacuum measurement. He is currently studying for his Ph.D. degree in the Institute of Electro-Optical Engineering of National Chiao Tung University. He is interested in the design and fabrication of micro-vacuum sensors and micromachining technology.

Yeong-Maw Chen received his B.S. degree in physics from National Central University of Taiwan in 1981, and his M.S. degree in electro-optical engineering from National Chiao Tung University in 1983. Since then he has been working in CSIST on radar system analysis and design. He is currently a Ph.D. candidate in the Institute of Electro-Optical Engineering of National Chiao Tung University, majoring in uncooled infrared detection.

Mang Ou-Yang received his B.S. degree in control engineering in 1991 and M.S. degree in electro-optical engineering in 1993 from National Chiao Tung University of Taiwan. He is currently a Ph.D. student in the same institute. His research is in the fabrication of thermal sensors and their readout electronics.

Jin-Shown Shie earned his B.S.E.E. degree from National Cheng Kung University in 1965 and M.S.E.E. degree from National Chiao Tung University in 1968, both in Taiwan. In 1972 he received his Ph.D. degree in materials sciences from SUNY at Stony Brook, USA. Since then he has joined the National Chiao Tung University and is currently a faculty member at the Institute of Electro-Optical Engineering. His current interest is in uncooled infrared FPA detectors and their system.